Development of fibrous PLGA/fibrin scaffolds as a potential skin substitute

To cite this article before publication: Juliana Girón *et al* 2020 *Biomed. Mater.* in press https://doi.org/10.1088/1748-605X/aba086

Development of fibrous PLGA/fibrin scaffolds as a potential skin substitute

Juliana Giron Bastidas (https://orcid.org/0000-0003-3131-5067) [1,2], Natasha Maurmann (https://orcid.org/0000-0001-5103-6394)[1,2], Mauro Ricardo da Silveira (http://orcid.org/0000-0001-9717-3036)[3], Carlos Arthur Ferreira (https://orcid.org/0000-0002-5707-8517) [3], Patricia Pranke (https://orcid.org/0000-0003-4698-6314) [1,2,4]

[1] Hematology & Stem Cell Laboratory, Faculty of Pharmacy, Universidade Federal do Rio Grande do Sul, Porto Alegre, RS, 90610-000, Brazil
[2] Post Graduate Program in Physiology, Universidade Federal do Rio Grande do Sul, Porto Alegre, RS, 90050-170, Brazil
[3] Engineering School. Universidade Federal do Rio Grande do Sul, Porto Alegre, RS
[4] Stem Cell Research Institute, Porto Alegre, RS, 90020-10, Brazil

The aim of this study has been to fabricate a hybrid electrospun nanofibrous scaffold composed of PLGA/fibrin polymers to be used as a skin substitute and analyze its physical and biological properties. Fibrin (Fib) was obtained from rat blood plasma, characterized and solubilized in formic acid. The final electrospinning solution concentration was 40 % PLGA (w/v) and 1 % fibrin (w/v). To improve spinnability, 3 % PEG (w/v) was added. The scaffolds were characterized by scanning electron microscopy (SEM) and Fourier-transform infrared spectroscopy (FTIR). Water contact angle, maximum elongation, thermal stability, degree of swelling, blood compatibility, cytotoxicity and cell viability were analyzed. The characterization by SEM showed randomly oriented nanofibers with a mean diameter of 639.8 ± 241.8 nm for the PLGA/Fib and 1051.0 ± 290.2 nm for the PLGA. FTIR spectra confirmed the presence of fibrin in the mats. Fibrin incorporation reduced the water contact angle from 118.9 ± 2.9 to 111.1 ± 2.8. The fibrin increased tensile strength and decreased elongation at break. The scaffolds demonstrated blood compatibility and fibrin incorporation improved cell adhesion and viability when direct and indirect MTT analyses were carried out. Thus, it can be concluded that the PLGA/fibrin mat is a promising material for use as a skin substitute.

Keywords: electrospinning; poly(lactic-co-glycolic) acid; fibrin.

1. Introduction

Skin is the largest organ of the body, with a surface of 2 m^2, this being a physical barrier between external and internal environments. It offers protection from dehydration, external damage, infections, UV radiation and environmental toxins. Furthermore, skin acts as a sensory organ, which transmits sensation to pain, temperature and deep pressure, playing an important role in the balance of body temperature and water content and, consequently, in the maintenance of physiological homeostasis (1). Skin is also one of the most immune active organs and interferes in vitamin D production, essential for calcium absorption and normal bone metabolism (2).

Skin disease prevalence has rapidly increased since 2005, with chronic wounds being a growing problem worldwide (3). Due to the importance of preserving skin integrity, tissue engineering has become an alternative to the conventional treatments for full-thickness wounds, which consist of the use of autografts, allografts or xenografts. These conventional treatments have some disadvantages, such as the risk of disease transmission, high cost and donor site morbidity (4).

One of the elements of tissue engineering which are of important relevance are the scaffolds, consisting of biomaterials fabricated from polymers of natural or synthetic origin which supports the cells. Their importance lies in the fact that the composition and structure of such biomaterials can provide appropriate conditions for the tissue regeneration process. Therefore, scaffolds act as an extracellular matrix analog; capable of guiding cell adhesion, proliferation and differentiation and also the promotion of angiogenesis. Such cell functions are influenced by polymer composition and related mechanical properties, including thickness and pore size (5).

Although tissue engineering of the skin has been widely studied, an ideal skin substitute has still not been developed. For a skin substitute to be considered ideal, it must have characteristics

such as water loss prevention because a moist wound environment is required to facilitate the healing process (6). However, adequate moisture balance is necessary. The water absorption capacity of the scaffolds, therefore, should be in agreement with the quantity of the wound exudate, it being possible to maintain a healthy physiological level of moisture (7). Thereby, dry wounds will require a hydrating scaffold, and in contrast, wounds with excessive exudate will require an absorptive scaffold able to prevent the maceration of the surrounding skin. Absorptive scaffolds should be able to transmit moisture vapor away from the wound bed towards the upper surface and allow the moisture to evaporate into the air. The transmission of moisture vapor is directly proportional to the porosity of the scaffold (8). Therefore, the scaffold should prevent dehydration and also the accumulation of extra exudates, such as seroma. For these reasons, the election of the scaffolds should be in agreement with the characteristics of the wound. On the other hand, complications like hematomas should be avoided by having good homeostasis before applying the substitute.

Besides water loss balance, characteristics such as a wide availability of the polymer, biodegradability, support for cellular adhesion, infection resistance, presence of epidermal and dermal components, low antigenicity, high shear strength, easy storage, long shelf life and good cost-benefit are desirable (5). These characteristics are dependent on the polymer properties and the technique used for scaffold fabrication. In this study, electrospinning was applied, which is a versatile technique widely used for fabricating fibers ranging from the nano- to the microscale.

In addition, the use of hybrid materials has been suggested in order to take advantage of the physical properties of synthetic polymers as well as the biological ones of natural polymers (9). Fibrin is a natural polymer composed of fibrinogen monomers present in blood plasma, with interesting properties to be used in tissue engineering which play an important role in the wound healing process. Fibrin acts as a support for the hemostatic plug and it is also considered to be a preliminary matrix within the wound space (10). Fibrin can interact with cells such as leukocytes, platelets, endothelial cells and fibroblast via integrin receptors. Arg-Gly-Asp (RGD) motif is the principal integrin-binding domain of ECM proteins, which play an important role in

cell adhesion (11). It has been shown that the fibrinogen molecules themselves (constituent A alpha and B beta chains) promote fibroblast proliferation (12).

Fibrin not only interacts with cells but also contains motifs that allow for the interaction with other ECM proteins, providing an adequate environment for cell adhesion, proliferation and migration (13). Native collagen I has binding sites that are common for fibrin, fibronectin and metalloproteinase 1 (14). This fact presupposes that a scaffold containing fibrin could provide a functional articulation between itself and the native tissue, therefore facilitating cell migration. Moreover, there are other ECM proteins capable of binding fibrin and regulating cell adhesion, proliferation and migration, such as fibronectin, vitronectin and thrombospondin (13) (11).

Furthermore, fibrin is an important signalizing molecule, being a potent vascular endothelial cell activator, inducing the expression of the IL8, which influence leukocyte migration and activation (11). It has also been reported that fibrin degradation product D-dimer induces synthesis and the release of IL-1β, IL-6 and plasminogen activator inhibitors from monocytes *in vitro*, which are regulators of hepatic response. IL-6 stimulates transcription of acute-phase proteins genes and fibrinogen synthesis, meanwhile, IL-1 down-regulates fibrinogen synthesis; which means that fibrin plays an active role in the tissue regeneration/repair processes (15).

Additionally, poly(lactic-co-glycolic) acid (PLGA) is a synthetic polymer approved by the European Medicine Agency as well as the US Food and Drugs Administration. PLGA is frequently used worldwide for biomedical applications and drug delivery as it is biodegradable, biocompatible and its degradation products are easily metabolized through the Krebs Cycle (16).

The aim of this study has been to produce electrospun nanofibrous scaffolds composed of PLGA/fibrin polymers and to analyze their physical and biological properties.

2. Materials and methods

2.1 Materials

The products used from Sigma-Aldrich were 1,1,1,3,3,3-hexafluoro2-propanol (HFIP), 3-(4, 5-dimethylthiazol-2-yl)-2,5-diphenyl tetrazolium bromide (MTT), 4,6-diamidino-2-phenylindole (DAPI), Dulbecco's Modified Eagle's Medium (DMEM/HEPES) - low glucose and high glucose, paraformaldehyde (PFA), rhodamine-phalloidin, trypsin-EDTA solution 10x and Triton X-100. Formic acid was purchased from Labsynth. Collagenase and penicillin/streptomycin were purchased from Gibco, PLGA 75:25 from PURAC, Fetal Bovine Serum (FBS) heat-inactivated from Cultilab, Campinas/SP and dimethyl sulfoxide (DMSO) from Nuclear.

2.2 Fibrin obtention and characterization

7 male Wistar rats aged 4 months (300–450 g body weight) were obtained from the Animal House of the Institute of Basic Health Sciences of the Federal University of Rio Grande do Sul. All the procedures were performed following authorization from the Ethics Committee (Number 36484, approved on 16th May, 2019).

The blood was collected after anesthesia with citrate-phosphate-dextrose anticoagulant in a 9:1 proportion by cardiac puncture. The harvested blood was centrifuged (800 *g*, 13 min at 4 °C) and the blood plasma was removed by aspiration, Fig 1. Fibrinogen polymerization was induced by adding 2.5 % $CaCl_2$ to the plasma (1:9). The plasma was incubated until clot formation; the clot was placed between two 0.2 µm pore size membranes and weight was applied until the formation of a thin sheet of fibrin. The fibrin was dehydrated at 37 °C for 48 hours. The dehydrated product was analyzed by Fourier transform infrared spectroscopy.

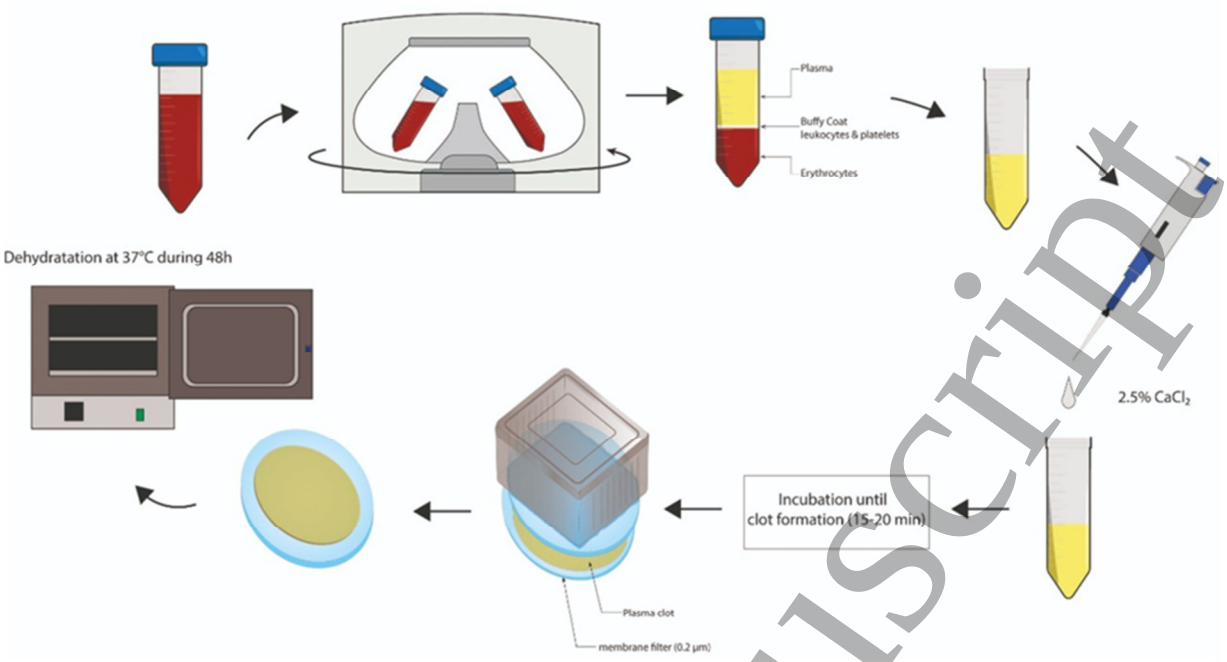

Fig. 1. Schematic process for fibrin obtention.

2.3 Preparation of electrospinning solution

Fibrin was dissolved in formic acid at room temperature with continuous stirring overnight at 1000 rpm. Once fibrin was dissolved, HFIP was added at the proportion of formic acid:HFIP 1:1. The solution was stirred for 15 minutes before adding the PLGA in a final solution concentration of 40 % PLGA (w/v), 1 % fibrin (w/v) and 3 % PEG (w/v). To dissolve the PLGA, the solution was stirred for 2 hours at room temperature until homogenization was reached. The electrospinning solution for the control scaffolds was prepared with the same solvents and solute concentration, with the exception of the fibrin.

2.4 Fabrication of PLGA and PLGA/fibrin electrospun nanofibers

The polymeric solution was loaded in a 2 ml plastic syringe fitted with a 23 G needle. The electrospinning parameters were fixed as applied high-voltage of 17 kV (18 kV at the positive and 1 kV at the negative) the flow rate of 0.48 ml/h controlled by a syringe pump (electrospinning model homemade) and a tip-collector distance of 20 cm. Random fibers were

electrospun on round glass coverslips of 13 mm diameter and were fixed using the same polymer solution prepared for the nanofibers fabrication on the underside of the glass coverslips so that they could be manipulated without distorting the microstructure. The scaffolds were sterilized with UV light for 1 hour at each site in a laminar flow hood.

2.5 Characterization

2.5.1 Scanning electron microscopy

The scaffold morphology and PLGA/Fib fiber diameter, together with the cell presence, were performed by the SEM model Pro X (Phenom-World – Thermo Fisher Scientific, the Netherlands). The samples were washed with phosphate buffer (PBS, pH 7.4), fixed in 4 % PFA for 30 minutes, rinsed in buffer PBS and dehydrated in ethanol series. The dried samples were metalized with a thin layer of gold and placed on stubs using adhesive carbon disks. Images were acquired using an accelerating voltage of 15 kV and a magnification range of 500–5,000×. The average fiber diameter was determined by SEM through the measurement of a total of 200 fibers of PLGA and PLGA/Fib, selected randomly from 7 images for each, using the ImageJ software.

2.5.2 Thermal stability and water contact angle

Thermal stability of the scaffolds and residual solvent content was evaluated by a thermogravimetric analyzer (TGA Q50, TA Instruments, USA), at a heating rate of 20 °C/min, in a temperature range of 30-800 °C under a nitrogen atmosphere. To analyze hydrophilicity, the water drop contact angle was carried out by Phoenix Mini (Surface & Electro-Optics Co., South Korea) using a sessile drop method (between 0.03 ml and 0.05 ml of drop volume), and a minimum of 15 drop images were recorded for each sample.

2.5.3 Mechanical testing

Maximum elongation and stress were determined by dynamic mechanical analysis (DMA) in a DMA 2980 (TA Instruments, USA) using the tension film clam. The scaffolds were cut into rectangular shapes (10×6 mm). The assays were carried out at a constant temperature (37 °C) with a ramp force of 0.1 N/min until 13 N maximum loads. Data from the stress-strain curves were recorded and the tensile stress at maximal load was obtained from this data for each sample. The analyses were made using the TA Universal Analysis software.

2.5.4 Fourier transform infrared spectroscopy

Influences of fibrin in the PLGA scaffolds were analyzed in the fingerprint region in the range of 2000 and 750 cm^{-1} in a FTIR spectrometer Spectrum 1000 (PerkinElmer, Inc., USA) by averaging 32 scans at a resolution of 4 cm^{-1}. The horizontal ATR (HATR) accessory (Pike Technologies, USA) was used for the PGLA and PLGA/Fib films; the fibrin powder was mixed with potassium bromide (KBr) (Sigma-Aldrich, USA) and pressed into a disk shape.

2.5.5 Swelling test

The scaffolds were cut into quadrangular shapes (1 cm x 1 cm) and weighed (W_i). To calculate the swelling degree, the membranes were immersed in PBS at 37 °C. After 1 hour and 24 hours, the scaffolds were removed and the surface water blotted out by filter paper to be weighed after swelling (W) (17). The swelling degree was calculated as follows:

$$Degree\ of\ Swelling\ (\%) = \frac{W - W_i}{W} x\ 100$$

2.5.6 Blood compatibility test

To test the compatibility of the scaffolds with blood, the hemolysis assay was performed. Citrated rat blood (4 ml) was diluted with 5 ml of normal saline 0.9 %. For the positive control, 10 ml of Milli-Q water was used and 10 ml of normal saline 0.9 % was taken as the negative

control. Scaffolds of diameter 1 cm were submerged in 10 ml of normal saline. Following this, 0.2 ml of citrated diluted blood was added to each group and incubated at 37 ºC for 60 minutes, followed by centrifugation at 1500 rpm for 10 minutes. Subsequently, the absorbance of the supernatant was taken at 570 nm. The hemolysis percentage was calculated as follows:

$$\% \, hemolysis = \frac{A_S - A_{NC}}{A_{PC} - A_{NC}}$$

Where A_S is the absorbance of the sample, A_{NC} is the absorbance of the negative control, A_{PC} is the absorbance of the positive control.

2.5.7 *In vitro* cell culture studies

Stem cells were isolated from exfoliated human deciduous teeth (SHED) (18) after approval by the Brazilian National Research Ethics Committee (Protocol number CAAE 12892419.0.0000.5347). SHED characterizations were performed by morphological analysis, flow cytometry, and differentiation assay *in vitro* (18–20).

To analyze cell viability on the scaffolds, the membranes were placed into a 24 well plate. SHED and HaCaT cells were seeded at a density of 25 x 10^3 cells per well and incubated at 37 °C with 5 % CO2. The culture media DMEM (low and high glucose for SHED and HaCaT, respectively) were supplemented with 10 % fetal bovine serum and 1 % penicillin/streptomycin. After 1 and 6 days, the cells were treated with 0.25 µg/ml of MTT for 4 hours at 37 °C. The supernatant was removed and 200 µl DMSO was added per well to dissolve the formed formazan crystals. The last procedure was made twice to obtain a good dissolution of the crystals. Absorbance was measured at 560 nm and 630 nm with the equipment Multiskan™ FC Microplate Photometer (Thermo Scientific™).

Cytotoxicity of the PLGA/Fib scaffolds was also analyzed by indirect MTT. The scaffolds were placed in a sterile tube and 1 ml of the culture medium with 1 % antibiotic without fetal bovine serum was added to each sterile sample. The scaffolds were incubated and after 7 days, the

scaffold incubated medium (SIM) was removed and supplemented with FBS 10 %. DMEM high glucose supplemented with FBS 10 % was considered as the control medium (CM). The cells (1600 HaCat per well) were seeded and cultivated in a 96-well plate and incubated for 8 hours to allow for the cells to adhere to the plate. After the incubation period, the culture medium was removed and 200 µl of SIM or CM was added to each well.

After 24 hours, the cell culture medium was removed and 50 µl of MTT with a concentration of 0.5 g/ml was added to each well. The plate was placed in a 5 % CO2 incubator at 37 °C for 2 hours. The media was then discarded and 200 µl DMSO was added to each well to dissolve the formazan crystals. The absorbance was measured at 570 nm. The toxicity and cell viability of the scaffold was calculated as follows:

$$Toxicity\ \ \%= \left(1 - \frac{mean\ of\ A_{SIM}}{mean\ of\ A_{CM}} \right) x\ 100 \qquad Viability\ \% = 100 - Toxicity\%$$

Where A_{SIM} is the absorbance of the cells treated with SIM and A_{CM} is the absorbance of the cells treated with the control medium.

2.5.8 Cell adhesion and morphology

The presence of cells attached to the nanostructured scaffolds was confirmed by fluorescence microscopy. The scaffolds were analyzed on the 1st and 6th days after the keratinocytes and SHED were seeded on the membranes. The membranes were washed in PBS, fixed in 4 % paraformaldehyde buffer for 30 minutes, rinsed in buffer PBS and the cell nuclei were blue stained with 0.5 µg/ml of DAPI (1 minute). To evaluate the morphology, the cells were stained with phalloidin (30 µg/ml) for actin filaments. The photographs were obtained by fluorescence microscope Leica DMi8 (Leica Microsystems).

3. Results and discussion

3.1 Morphology and diameter of the nanofibrous scaffolds

Fig. 2 shows by SEM the formation of randomly oriented nanofibers with heterogeneous diameters. The SEM images of the PLGA scaffolds are illustrated in Figs. 2a, b; the mean diameter of the fibers was 1051.0 ± 290.2 nm (Fig. e).

The PLGA/Fib scaffolds presented a diameter ranging from 200 nm to 1300 nm, with a mean of 639.8 ± 241.8 nm. Approximately 77 % of the fiber diameter was located between 300 and 800 nm (Figs. 2c, d, f). The smaller diameter in the PLGA/Fib scaffolds is probably related to the addition of $CaCl_2$ salt to the plasma, improving the electrical conductivity of the polymeric solution and, consequently, decreasing the fibers diameter (21).

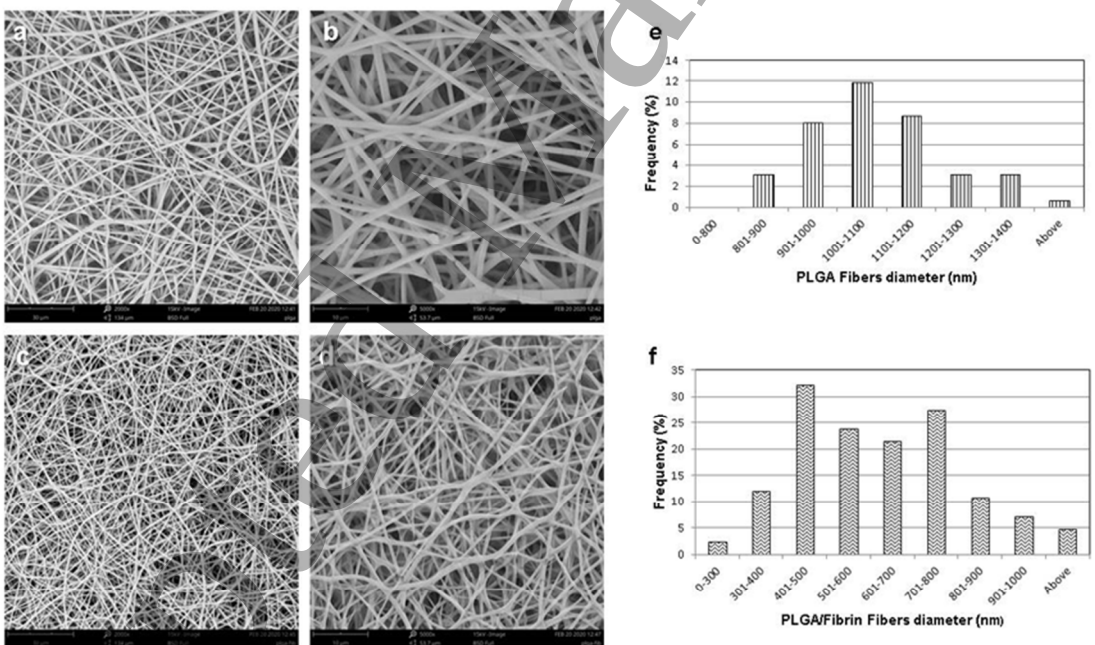

Fig. 2. SEM characterization for nanofibrous scaffolds. PLGA scaffold (a, b). PLGA/fibrin scaffold (c, d). Diameter distribution for PLGA scaffolds (e). Diameter distribution for PLGA scaffolds (f).

It is important to highlight that fibers with concentrations of PLGA lower than 40 % presented beads and it was necessary to increase their concentration for obtaining uniform fibers and to counteract the acidic hydrolytic effect of formic acid. Formic acid could be responsible for maintaining a higher percentage of fibers with a diameter in the nanoscale (22). On the other hand, it was observed that by increasing the concentration of the natural polymer, the fibers also presented beads; for this reason it was necessary to maintain a 1 % fibrin concentration. Formic acid has been used to improve the solubilization of natural polymer and to develop hybrid scaffolds; the presented results are consistent with the findings of other investigations when formic acid was used. Shalumon and colleagues developed a hybrid scaffold of chitosan and PCL using formic acid as a solvent, and to avoid the formation of beads, it was necessary to increase the concentration of the synthetic polymer and decrease the concentration of the natural one (23). However, studies using low concentrations of the natural polymer have already reported efficient results (24)(25)(26)(27), and in this study,, it is demonstrated that the incorporation of 1 % fibrin increases cell viability.

3.2 Thermal stability and water contact angle

The hydrophilicity of the nanofibrous membranes was analyzed by contact angle determination. The water contact angle of the PLGA scaffolds was 118.9 ± 2.9 (Fig. 3a); however, with the incorporation of fibrin, the water contact angle of the PLGA/Fib scaffolds decreased to 111.1 ± 2.8 (Fig. 3b). Although fibrin presents a moderated hydrophobic nature after fibrinogen polymerization, which is determined by acid-base and Van der Waals interactions, the water contact angle of the PLGA/fibrin scaffolds was reduced (28). While it can still be considered hydrophobic, a lower water contact angle could influence the improvement of cell-scaffold interaction.

To investigate the thermal stability of the PLGA/Fib scaffolds, TGA analysis was carried out. On the TGA curves (Fig. 3c) it is possible to see a shift of the curve to the left, which signifies that the incorporation of fibrin facilitates scaffold degradation.

The PLGA scaffold showed two decomposition events, the first between 30-100 °C, probably related to residual solvent evaporation (Table 1, Fig. 3d). The second event occurred between 100-500 °C when 98.3 % of the scaffold weight was lost; this is associated with thermal degradation of the polymer backbone, as seen in other investigations (29)(30).

The PLGA/fibrin scaffold showed four degradation events. The first event, related to the residual solvent, appears again between 30-100 °C, and 89.3 % of the scaffold weight had been lost between 100-380 °C. The third degradation event for the PLGA/Fib scaffold occurred between 380-450 °C, when 5.6 % of the weight was lost. This event is probably related to fibrin degradation.

The fibrin substrate presented slower degradation kinetics, with four degradation events. In this case, weight loss occurred gradually, without big peaks of degradation. The polymer had lost 62.8 % of its weight at 550 °C, and above this temperature, the final decomposition phase or carbonization of the polymer was observed (31). A residual product of 28.9 % at 800 °C was seen (Table 1, Fig. 3d). The result shows that isolated fibrin is a stable product with important intermolecular forces, and explains why in the PLGA/Fib scaffold there was a residual mass at 800 °C of 0.1 %, which is related to the natural polymer and its final carbonization phase (Table 1).

Furthermore, based on the experience of our research group working with PLGA 75:25, it has been observed that the molecular weight of electrospun PLGA scaffolds decreased about 32% after 45 days of incubation in PBS (32) and an *in vivo* partial degradation of the PLGA scaffold after 6 weeks was also observed, (33). On the other hand, biodegradation of fibrin is mediated by plasmin and it is subject to a variety of factors such as tissue metabolism rate, tissue depth, presence of cells and fibrinogen concentration (34). Wolbank and colleagues reported that the subcutaneous degradation kinetic for fibrin was of approximately 16 days (35). Similarly, other authors have reported fibrin degradation in between one and two weeks, depending on the addition or not of cells (36) (37) (38). It has therefore been suggested that, due to the degradation characteristics of PLGA spun scaffolds, they should be used for chronic wounds

(39). However, future studies should be made to determine the influence on the scaffold degradation behavior when 1% of fibrin is incorporated on PLGA mats.

Table 1. Characteristic degradation temperatures of PLGA/fibrin scaffolds and fibrin substrate

Sample	Events	Temperature Range (°C)	T max (°C)	Weight Loss (%)	Weight (%)				
					100 °C	300 °C	500 °C	700 °C	Residue at 800 °C
PLGA	1	30-100	72.3	0.32	99.68	96.08	1.38	0.02	0.0
	2	100-500	386.1	98.29					
	3	500-800	-------	1.39					
PLGA/Fib	1	30-100	72.1	2.31	97.69	85.63	2.26	0.26	0.1
	2	100-380	353.4	89.31					
	3	380-450	402.8	5.56					
	4	450-800	-------	2.72					
Fibrin	1	30-200	158.8	12.60	96.92	76.40	39.02	32.52	28.94
	2	200-360	320.6	30.88					
	3	360-550	375.4	19.28					
	4	550-800	-------	8.30					

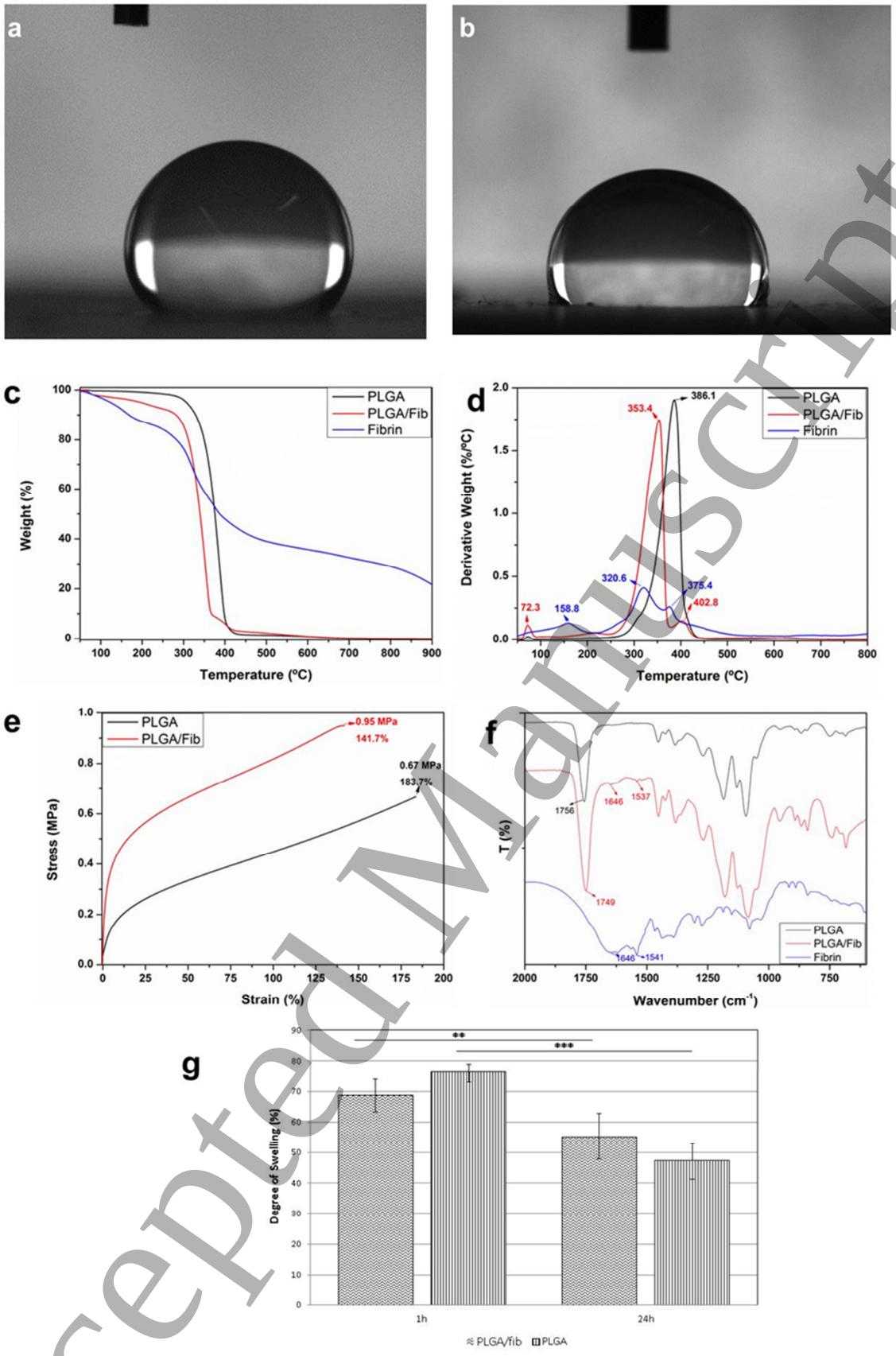

Fig. 3. Water contact angle for PLGA scaffold (a) and PLGA/fibrin scaffold (b). TGA thermograms (c). Derivative of the TGA curve (d). Stress-strain curves (e). Fourier transform infrared spectroscopy (f). Degree of swelling for scaffolds (g).

3.3 Mechanical properties of nanofiber scaffolds

Stress-strain curves of PLGA and PLGA/fib scaffolds are presented in Fig. 3e. The tensile strength of the scaffold increased when fibrin was incorporated, meanwhile, elongation at break decreased from 183.7 to 141.7 %. The increment of the tensile strength and decrease of elongation at break could be attributed to the fibrin's intramolecular hydrogen bonding properties, inducing bundle formation by reinforcing the PLGA fibers (24). Studies have found values of higher tensile strength and lower elongation at break for PLGA scaffolds, even with a lower concentration of the polymer (40)(41)(29), which indicates that the effect of formic acid on the polymer should be further studied.

Thus, it can be concluded that fibrin incorporation enhances the mechanical properties of the scaffold and such properties are expected to improve with the incorporation of cells and the gradual deposition of the extracellular matrix.

3.4 Fourier transform infrared spectroscopy of scaffolds

Influences of fibrin in the PLGA scaffolds were analyzed in the range between 2000 and 750 cm^{-1}. FTIR results are shown in Fig. 3f. The fibrin presented characteristic amide absorption peaks (N-H), including 1541 cm^{-1} (Amide II bond) and 1646 cm^{-1} (Amide I bond) (42)(43). PLGA displayed a characteristic absorption carbonyl (C=O) pick in 1756 cm^{-1} as well as a characteristic absorption band between 1100–1250, which represents the esters groups (C-O) (44). On the other hand, the PLGA/fibrin scaffold showed similar peaks of both fibrin and PLGA.

Although the association of fibrin with synthetic polymers using the electrospinning technique for the development of scaffolds has already been reported, these studies used commercial fibrinogen (45)(46) or purified fibrinogen (47), which incurs higher production costs. Some studies have supported the use of blood plasma, but in these cases, the intention has been of coating the electrospinning mats with fibrin (48)(49), and not including the natural polymer in the electrospinning solution.

The method used in this present study, therefore, is advantageous because of its simplicity and low-cost, it being possible to construct the mat with autologous plasma without the risk of rejection induced by the natural polymer.

3.5 Swelling behavior

The ability to absorb water is a relevant characteristic of a skin substitute because of the importance of preventing severe fluid loss in full-thickness injuries. This study calculated the swelling degree of the mats, to evaluate if the incorporation of fibrin could contribute to decreasing the swelling degree of the scaffold, taking into account that fibrin from a plasma blood clot is moderately hydrophobic (28). The results showed no statistically significant difference at the first hour for the PLGA and PLGA/fibrin scaffold, with a swelling degree of 76 ± 3 % and 69 ± 5 %, respectively Fig. 3g. However, after 24 hours, both mats presented a reduction in the swelling capacity of 55 ± 7 % for the PLGA/fibrin and 47 ± 6 % for the PLGA. Although the PLGA/fibrin swelling degree was better, the difference was not significant. The behavior of the membranes was expected due to the phenomenon of contraction that PLGA spun fibers undergo when mats are incubated in PBS at 37 °C, a phenomenon that has been widely reported (50)(51). The contraction forces of the polymer fibers could thus hinder the scaffold expansion caused by water absorption.

3.6 Blood compatibility

To evaluate if the PLGA/fibrin scaffold was compatible with blood, the hemolysis percentage was calculated. The hemolysis percentage denotes the ratio of erythrocytes, whose cell membrane is broken down when it comes into contact with the mat. Thus, a lower hemolysis percentage suggests good hemocompatibility of the scaffold. Fig. 4a illustrates the absorbance of the hemolysis assay. Absorbance for the positive control was 0.432 ± 0.012. Absorbance for the negative control, PLGA scaffold and PLGA/fibrin scaffolds was: 0.006 ± 0.001; 0.006 ±

0.001, and 0.006 ± 0.001, respectively, with hemolysis percentage for the PLGA and PLGA/fibrin scaffolds of 0.117 and 0.088, respectively. It can be concluded that both scaffolds were highly hemocompatible.

3.7 Indirect MTT Assay

To test the cytocompatibility and toxicity of the mats, an indirect MTT assay was performed. Fig. 4b shows increased cell viability of 107.2 ± 6.8 % in the cells cultivated with the SIM of PLGA/fibrin mats compared with the control (cells cultivated with DMEM supplemented with FBS 10 %). The results suggest that the SIM of the PLGA/fibrin scaffold contributed to improving the viability of the HaCaT cells, perhaps due to the fibrin release from the scaffold. On the other hand, the toxicity percentage of the PLGA/fibrin scaffold was: -7.2 %. A negative result was obtained due to the mean of the absorbance in the group of cells cultivated with SIM from the PLGA/fibrin scaffold being greater than that of the control.

3.8 Direct MTT Assay

MTT assay was used to evaluate the cell viability of the HaCaT and SHED cells on the scaffolds after 1 and 6 days. The tissue culture plate (TCP) was taken as control. Figs. 4c and d illustrate absorbances for each group at different times.

The results showed similar viability of the HaCaT cells on the PLGA/fibrin scaffolds compared with the TCP on the first day (Fig. 4c). In contrast, the PLGA scaffold promoted significantly reduced viability compared with the PLGA/fibrin scaffolds. On the sixth day, there was a significant difference in the HaCaT cell viability cultivated on the PLGA/fibrin scaffold compared with the PLGA scaffold, although, it was inferior to the TCP. The results suggest that the incorporation of fibrin influenced initial HaCaT adhesion and proliferation. Although it was described that keratinocytes are not able to bind to fibrin due to the lack of integrin αvβ3 (52), it has also been described that migration and proliferation of keratinocytes is dependent on fibrinogen concentration (53); fibrinogen concentration, therefore, ranging from 17–33 mg/ml in

fibrin 3D constructs provides an appropriate proliferation for keratinocytes. On the other hand, in the protein composition of a fibrin clot, fibronectin has been identified (43) (54), which has adhesion sites for α5β1 integrins, expressed in keratinocytes, being important for keratinocyte migration (55). Besides this, it has been suggested that fibrin stimulates keratinocytes to secrete TGF-α, which in turn increases cell proliferation and EGF receptor capacity, supporting the proliferation of keratinocytes in an autocrine fashion (56).

When SHED viability was evaluated, the results showed a significant difference between all the groups, both on day 1 and day 6 (Fig. 4d). On the first day, there was a significantly increased viability of SHEDs on the PLGA/fibrin scaffold compared to the PLGA scaffold; however, the viability in the TCP was superior. In contrast, on day 6, the PLGA/fibrin scaffold had a significantly increased viability compared to the TCP as well as the PLGA scaffold. The PLGA scaffold viability was significantly reduced when compared to the PLGA/fibrin scaffold and the TCP.

The results suggest that the incorporation of fibrin in the mats improved the biological properties of the PLGA polymer, and viability on the mats is cell type-dependent.

3.9 Cell adhesion and morphology

The nuclei of the cells were stained with DAPI to evaluate if the cells were able to adhere to the scaffolds after one day and, to evaluate the morphology, actin filaments were stained with phalloidin (Figs. 4e-j). The SHED cultivated on the PLGA/fibrin scaffolds (Fig. 4g) presented a similar conformation of their morphology comparable with the control group (Fig. 4e). Meanwhile, the SHED culture in the PLGA scaffolds stills exhibited rounded morphology (Fig. 4f). The HaCaT cells presented a similar cytoskeleton conformation in both the PLGA and PLGA/Fib scaffolds (Figs. 4i and j, respectively), being evident the presence of a higher cell density on the scaffold with fibrin incorporation. Images were taken in sites of greater cellular confluence.

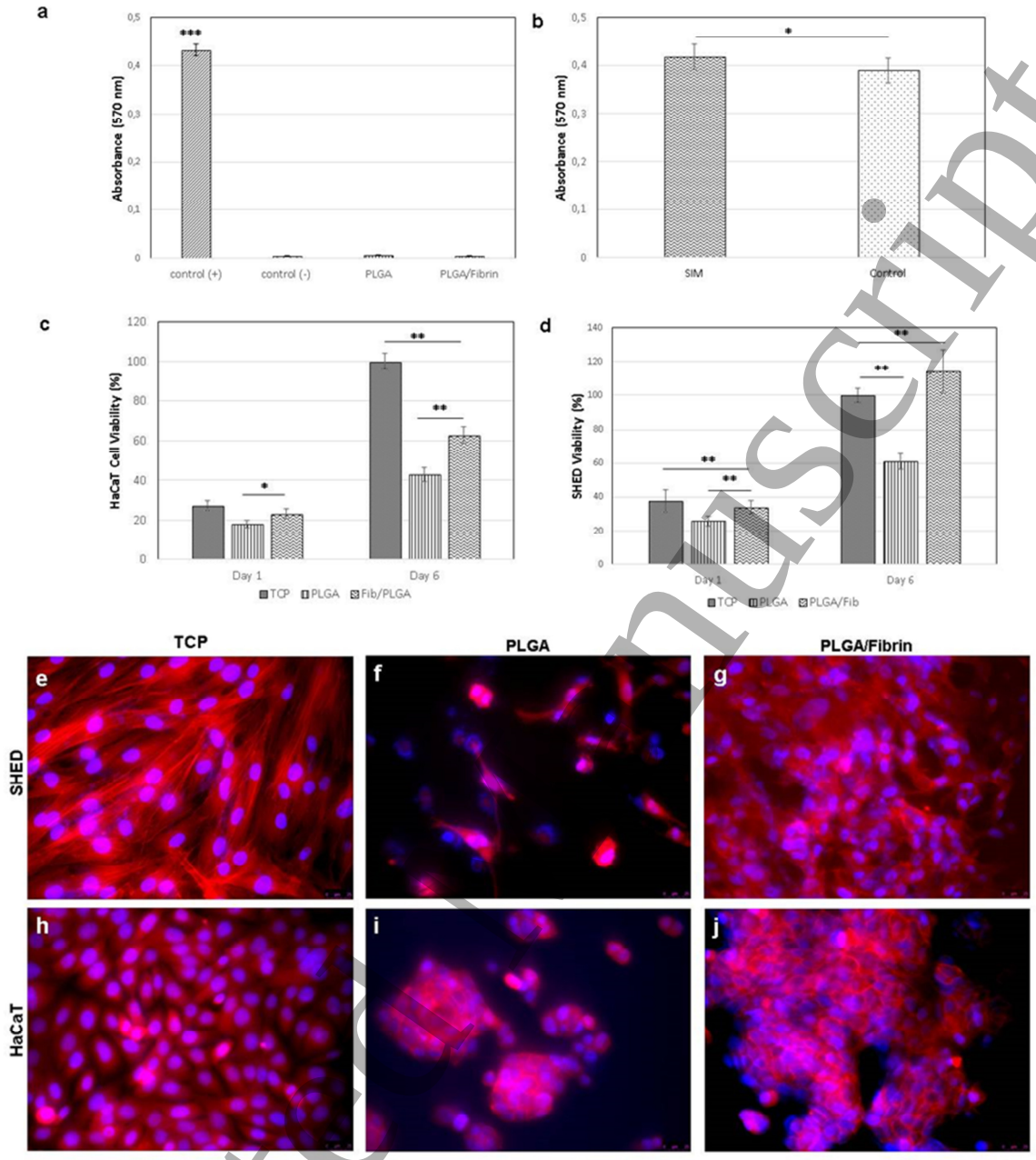

Fig. 4. Hemolysis assay for scaffolds (a). Indirect MTT assay (b). MTT assay of scaffolds using HaCaT cells at days 1 and day 6 (c). MTT assay of scaffolds using SHED cells at days 1 and day 6 (d). DAPI and phalloidin stain on scaffolds at day 1, with 400x magnification using SHED (e, f, g) and HaCaT cells (h, i, j).

The images taken at day six with DAPI stain are shown in Figs. 5a-f. Magnification 200x shows an overview of cell density on day 6, which confirms the results shown in the MTT assay. A higher nuclei density for both cell types in the PLGA/fibrin scaffolds can be seen compared with the PLGA scaffolds (Figs. 5c and 5f).

As seen in the DAPI stain images, the SEM images of 500x magnification (Figs. 5g, i, k, and m) showed a greater cell number in both cell types cultivated in the scaffolds with fibrin incorporation. It is even possible to see a layer of HaCaT cells on the PLGA/fibrin scaffold (Fig 5m), meanwhile, scattered cells are seen in the PLGA scaffolds (Fig. 5k). The images with 2000x magnification (Figs. 5h, j, l, n) show a normal morphology of both cell types at day six, on both the PLGA and PLGA/fibrin scaffolds.

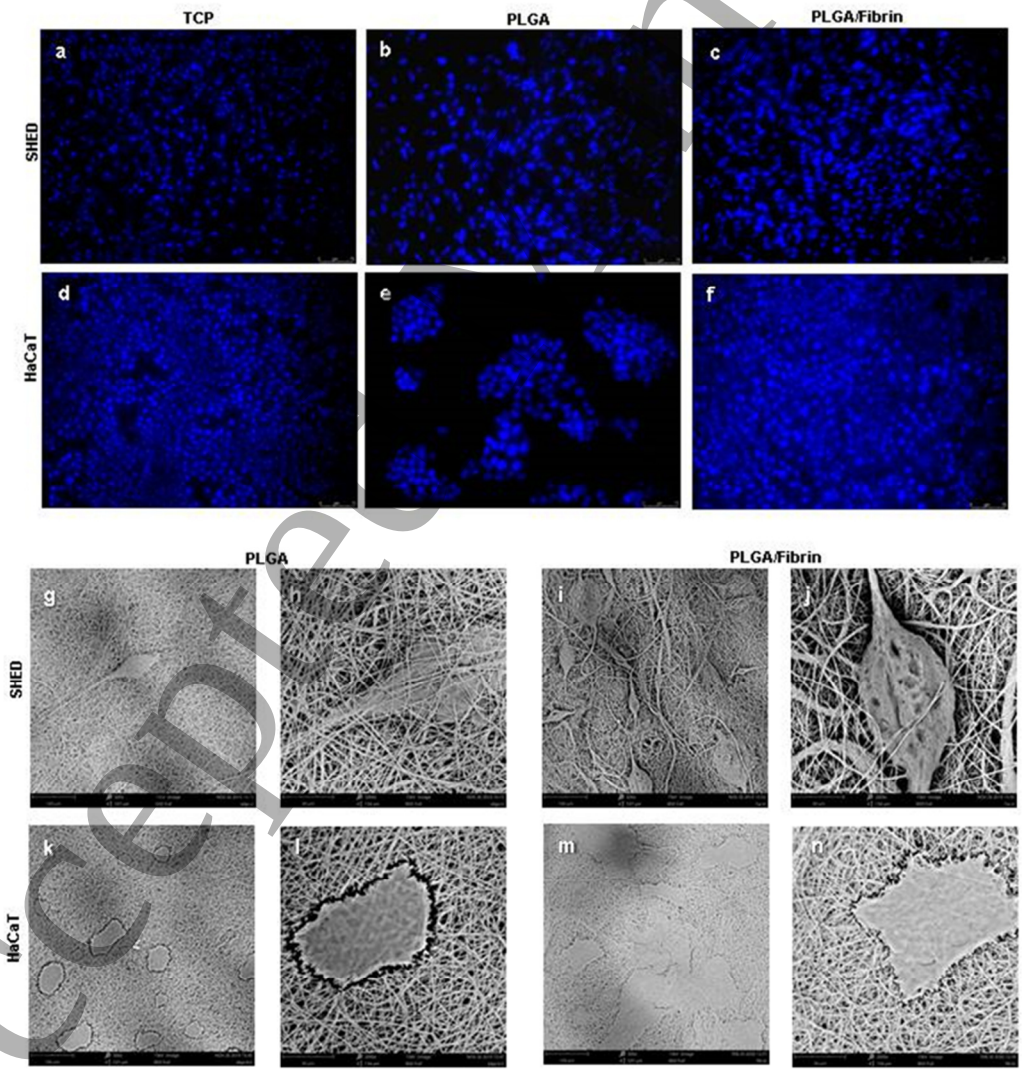

Fig. 5. DAPI staining cell nuclei on scaffolds at day 6, with 200x magnification using SHED (a, b, c) and HaCaT cells (d, e, f). SEM images for scaffolds cultivated with cells at day 6, using SHED (g, h, i, j) and HaCaT cells (k, l, m, n).

4. Conclusion

In the present investigation, nanofibrous hybrid scaffolds of PLGA synthetic polymer and fibrin natural polymer were produced. It was demonstrated that the incorporation of 1 % fibrin allows for the production of material with enhanced mechanical properties and cell viability as well as good blood compatibility. Furthermore, the isolation method of fibrin was shown to be a simple and efficient method for the obtainment of fibrin and probably other plasma proteins, which improve the biological properties of PLGA scaffolds. It can therefore be suggested that fibrin could be used for spinning other synthetic polymers, considering the poor biological properties of such materials. Finally, it can be concluded that the PLGA/fibrin scaffold is a promising material to be used as a skin substitute.

Funding: This work was supported by *Coordenação de Aperfeiçoamento de Pessoal de Nível Superior* (CAPES) for Ph.D. fellowship, Brazil [grant numbers 88882.439513/2019-01, 2019]; Ministry of Science, Technology, Innovations and Communications (MCTIC)/FEEG/FURGS, Brazil [grant number 23078.010846/2019-78]; *Financiadora de Estudos e Projetos* (FINEP), [grant number 0114013500]; *Fundação de Amparo à Pesquisa do Estado do Rio Grande do Sul* (FAPERGS), [grant number 17/255/0001271-2] and Research the Stem Cell Research Institute.

References

1. Matejuk A. Skin Immunity. Vol. 66, Archivum Immunologiae et Therapiae Experimentalis. Birkhauser Verlag AG; 2018. p. 45–54.
2. Guttman-Yassky E, Zhou L, Krueger JG. The skin as an immune organ: Tolerance versus effector responses and applications to food allergy and hypersensitivity reactions. J Allergy Clin Immunol. 2019 Aug 1;144(2):362–74.
3. Vos T, Allen C. Global, regional, and national incidence, prevalence, and years lived with disability for 310 diseases and injuries, 1990–2015: a systematic analysis for the Global Burden of Disease Study 2015. Lancet. 2016 Oct 8;388(10053):1545–602.
4. Paggiaro AO, Bastianelli R, Carvalho VF, Isaac C, Gemperli R. Is allograft skin, the gold-standard for burn skin substitute? A systematic literature review and meta-analysis. Vol. 72, Journal of Plastic, Reconstructive and Aesthetic Surgery. Churchill Livingstone; 2019. p. 1245–53.
5. Nicholas MN, Jeschke MG, Amini-Nik S. Methodologies in creating skin substitutes. Vol. 73, Cellular and Molecular Life Sciences. Birkhauser Verlag AG; 2016. p. 3453–72.
6. Winter GD. Formation of the scab and the rate of epithelization of superficial wounds in the skin of the young domestic pig. Nature. 1962;193(4812):293–4.
7. Jaffe L, Wu SC. Dressings, Topical Therapy, and Negative Pressure Wound Therapy. Vol. 36, Clinics in Podiatric Medicine and Surgery. W.B. Saunders; 2019. p. 397–411.
8. Sobhanian P, Khorram M, Hashemi SS, Mohammadi A. Development of nanofibrous collagen-grafted poly (vinyl alcohol)/gelatin/alginate scaffolds as potential skin substitute. Int J Biol Macromol. 2019 Jun 1;130:977–87.
9. Pina S, Ribeiro VP, Marques CF, Maia FR, Silva TH, Reis RL, et al. Scaffolding Strategies for Tissue Engineering and Regenerative Medicine Applications. Materials

(Basel) [Internet]. 2019 Jun 5 [cited 2020 Feb 19];12(11):1824. Available from: https://www.mdpi.com/1996-1944/12/11/1824

10. Kordestani SS. Wound Healing Process. In: Atlas of Wound Healing. Elsevier; 2019. p. 11–22.

11. Sproul E, Nandi S, Brown A. Fibrin biomaterials for tissue regeneration and repair. In: Peptides and Proteins as Biomaterials for Tissue Regeneration and Repair. Elsevier Inc.; 2017. p. 127–50.

12. Gray AJ, Bishop JE, Reeves JT, Laurent GJ. A alpha and B beta chains of fibrinogen stimulate proliferation of human fibroblasts. J Cell Sci [Internet]. 1993 Feb [cited 2020 Feb 19];104 (Pt 2):409–13. Available from: http://www.ncbi.nlm.nih.gov/pubmed/8505369

13. Heher P, Mühleder S, Mittermayr R, Redl H, Slezak P. Fibrin-based delivery strategies for acute and chronic wound healing. Vol. 129, Advanced Drug Delivery Reviews. Elsevier B.V.; 2018. p. 134–47.

14. Reyhani V, Seddigh P, Guss B, Gustafsson R, Rask L, Rubin K. Fibrin binds to collagen and provides a bridge for αVβ3 integrin-dependent contraction of collagen gels. Biochem J [Internet]. 2014 Jul 15 [cited 2020 Feb 19];462(1):113–23. Available from: http://www.ncbi.nlm.nih.gov/pubmed/24840544

15. Robson SC, Shephard EG, Kirsch RE. Fibrin degradation product D-dimer induces the synthesis and release of biologically active IL-1β, IL-6 and plasminogen activator inhibitors from monocytes in vitro. Br J Haematol [Internet]. 1994 Feb 1 [cited 2020 Feb 19];86(2):322–6. Available from: http://doi.wiley.com/10.1111/j.1365-2141.1994.tb04733.x

16. Maurmann N, Sperling LE, Pranke P. Electrospun and Electrosprayed Scaffolds for Tissue Engineering. In: Advances in Experimental Medicine and Biology. Springer New York LLC; 2018. p. 79–100.

17. Sobhanian P, Khorram M, Hashemi SS, Mohammadi A. Development of nanofibrous

collagen-grafted poly (vinyl alcohol)/gelatin/alginate scaffolds as potential skin substitute. Int J Biol Macromol. 2019 Jun 1;130:977–87.

18. Descripción: Efeito da remoção seletiva de tecido cariado nas características imunofenotípicas apresentadas por células-tronco mesenquimais da polpa de dentes decíduos humanos [Internet]. [cited 2020 Feb 24]. Available from: http://oasisbr.ibict.br/vufind/Record/URGS_244b5d1cd1810559e5320b1fde9b64b8/Description#tabnav

19. Maurmann N, Pereira DP, Burguez D, Pereira FDADS, Neto PI, Rezende RA, et al. Mesenchymal stem cells cultivated on scaffolds formed by 3D printed PCL matrices, coated with PLGA electrospun nanofibers for use in tissue engineering. Biomed Phys Eng Express. 2017;3(4).

20. Siqueira RL, Maurmann N, Burguêz D, Pereira DP, Rastelli ANS, Peitl O, et al. Bioactive gel-glasses with distinctly different compositions: Bioactivity, viability of stem cells and antibiofilm effect against Streptococcus mutans. Mater Sci Eng C. 2017;76.

21. Mehdikhani M, Ghaziof S. Electrically conductive poly- ϵ -caprolactone/polyethylene glycol/multi-wall carbon nanotube nanocomposite scaffolds coated with fibrin glue for myocardial tissue engineering. Appl Phys A Mater Sci Process. 2018 Jan 1;124(1):1–15.

22. Van Der Schueren L, De Schoenmaker B, Kalaoglu ÖI, De Clerck K. An alternative solvent system for the steady state electrospinning of polycaprolactone. Eur Polym J. 2011 Jun 1;47(6):1256–63.

23. Shalumon KT, Anulekha KH, Girish CM, Prasanth R, Nair S V., Jayakumar R. Single step electrospinning of chitosan/poly(caprolactone) nanofibers using formic acid/acetone solvent mixture. Carbohydr Polym. 2010 Apr 12;80(2):413–9.

24. Türker E, Yildiz ÜH, Arslan Yildiz A. Biomimetic hybrid scaffold consisting of co-electrospun collagen and PLLCL for 3D cell culture. Int J Biol Macromol. 2019 Oct 15;139:1054–62.

25. Mahsa Khatami S, Parivar K, Naderi Sohi A, Soleimani M, Hanaee-Ahvaz H. Acetylated hyaluronic acid effectively enhances chondrogenic differentiation of mesenchymal stem cells seeded on electrospun PCL scaffolds. Tissue Cell [Internet]. 2020 Apr 11 [cited 2020 Apr 15];101363. Available from: https://linkinghub.elsevier.com/retrieve/pii/S0040816619305221

26. Kenar H, Ozdogan CY, Dumlu C, Doger E, Kose GT, Hasirci V. Microfibrous scaffolds from poly(L-lactide-co-ε-caprolactone) blended with xeno-free collagen/hyaluronic acid for improvement of vascularization in tissue engineering applications. Mater Sci Eng C. 2019 Apr 1;97:31–44.

27. Eskandarinia A, Kefayat A, Gharakhloo M, Agheb M, Khodabakhshi D, Khorshidi M, et al. A propolis enriched polyurethane-hyaluronic acid nanofibrous wound dressing with remarkable antibacterial and wound healing activities. Int J Biol Macromol. 2020 Apr 15;149:467–76.

28. van Oss CJ. Surface properties of fibrinogen and fibrin. J Protein Chem. 1990 Aug;9(4):487–91.

29. Li AD, Sun ZZ, Zhou M, Xu XX, Ma JY, Zheng W, et al. Electrospun Chitosan-graft-PLGA nanofibres with significantly enhanced hydrophilicity and improved mechanical property. Colloids Surfaces B Biointerfaces. 2013 Feb 1;102:674–81.

30. Li J, Zhu J, He T, Li W, Zhao Y, Chen Z, et al. Prevention of intra-abdominal adhesion using electrospun PEG/PLGA nanofibrous membranes. Mater Sci Eng C. 2017 Sep 1;78:988–97.

31. Natarajan D, Kiran MS. Fabrication of juglone functionalized silver nanoparticle stabilized collagen scaffolds for pro-wound healing activities. Int J Biol Macromol. 2019 Mar 1;124:1002–15.

32. Braghirolli DI, Zamboni F, Acasigua GAX, Pranke P. Association of electrospinning with electrospraying: A strategy to produce 3D scaffolds with incorporated stem cells for use in tissue engineering. Int J Nanomedicine. 2015 Aug 14;10:5159–70.

33. Reis KP, Sperling LE, Teixeira C, Paim Á, Alcântara B, Vizcay-Barrena G, et al. Application of PLGA/FGF-2 coaxial microfibers in spinal cord tissue engineering: an *in vitro* and *in vivo* investigation. Regen Med [Internet]. 2018 Oct 1 [cited 2020 Jun 10];13(7):785–801. Available from: https://www.futuremedicine.com/doi/10.2217/rme-2018-0060

34. Anitua E, Nurden P, Prado R, Nurden AT, Padilla S. Autologous fibrin scaffolds: When platelet- and plasma-derived biomolecules meet fibrin. Vol. 192, Biomaterials. Elsevier Ltd; 2019. p. 440–60.

35. Wolbank S, Pichler V, Ferguson JC, Meinl A, van Griensven M, Goppelt A, et al. Non-invasive *in vivo* tracking of fibrin degradation by fluorescence imaging. J Tissue Eng Regen Med [Internet]. 2015 Aug 1 [cited 2020 Jun 12];9(8):973–6. Available from: http://doi.wiley.com/10.1002/term.1941

36. Breidenbach AP, Dyment NA, Lu Y, Rao M, Shearn JT, Rowe DW, et al. Fibrin gels exhibit improved biological, structural, and mechanical properties compared with collagen gels in cell-based tendon tissue-engineered constructs. Tissue Eng - Part A. 2014 Feb 1;21(3–4):438–50.

37. Anitua E, Zalduendo MM, Prado R, Alkhraisat MH, Orive G. Morphogen and proinflammatory cytokine release kinetics from PRGF-Endoret fibrin scaffolds: Evaluation of the effect of leukocyte inclusion. J Biomed Mater Res Part A [Internet]. 2015 Mar 1 [cited 2020 Jun 12];103(3):1011–20. Available from: http://doi.wiley.com/10.1002/jbm.a.35244

38. Neuss S, Schneider RKM, Tietze L, Knüchel R, Jahnen-Dechent W. Secretion of Fibrinolytic Enzymes Facilitates Human Mesenchymal Stem Cell Invasion into Fibrin Clots. Cells Tissues Organs [Internet]. 2010 Jan [cited 2020 Jun 12];191(1):36–46. Available from: https://www.karger.com/Article/FullText/215579

39. Vázquez N, Sánchez-Arévalo F, Maciel-Cerda A, Garnica-Palafox I, Ontiveros-Tlachi R, Chaires-Rosas C, et al. Influence of the PLGA/gelatin ratio on the physical, chemical

and biological properties of electrospun scaffolds for wound dressings. Biomed Mater. 2019 May 7;14(4):045006.

40. Eren Boncu T, Uskudar Guclu A, Catma MF, Savaser A, Gokce A, Ozdemir N. In vitro and in vivo evaluation of linezolid loaded electrospun PLGA and PLGA/PCL fiber mats for prophylaxis and treatment of MRSA induced prosthetic infections. Int J Pharm. 2020 Jan 5;573:118758.

41. Luo H, Zhang Y, Gan D, Yang Z, Ao H, Zhang Q, et al. Incorporation of hydroxyapatite into nanofibrous PLGA scaffold towards improved breast cancer cell behavior. Mater Chem Phys. 2019 Mar 15;226:177–83.

42. Deepthi S, Abdul Gafoor AA, Sivashanmugam A, Nair S V., Jayakumar R. Nanostrontium ranelate incorporated injectable hydrogel enhanced matrix production supporting chondrogenesis: In vitro. J Mater Chem B. 2016 Jun 8;4(23):4092–103.

43. Litvinov RI, Faizullin DA, Zuev YF, Weisel JW. The α-helix to β-sheet transition in stretched and compressed hydrated fibrin clots. Biophys J. 2012 Sep 5;103(5):1020–7.

44. Sadeghi-Avalshahr A, Nokhasteh S, Molavi AM, Khorsand-Ghayeni M, Mahdavi-Shahri M. Synthesis and characterization of collagen/PLGA biodegradable skin scaffold fibers. Regen Biomater. 2017 Oct 1;4(5):309–14.

45. Law JX, Musa F, Ruszymah BHI, El Haj AJ, Yang Y. A comparative study of skin cell activities in collagen and fibrin constructs. Med Eng Phys. 2016 Sep 1;38(9):854–61.

46. Baker S, Sigley J, Helms CC, Stitzel J, Berry J, Bonin K, et al. The mechanical properties of dry, electrospun fibrinogen fibers. Mater Sci Eng C. 2012 Feb 1;32(2):215–21.

47. Li S, Su L, Li X, Yang L, Yang M, Zong H, et al. Reconstruction of abdominal wall with scaffolds of electrospun poly (L-lactide-co caprolactone) and porcine fibrinogen: An experimental study in the canine. Mater Sci Eng C. 2020 May 1;110:110644.

48. Malikmammadov E, Tanir TE, Kiziltay A, Hasirci N. Preparation and characterization of

poly(ε-caprolactone) scaffolds modified with cell-loaded fibrin gel. Int J Biol Macromol. 2019 Mar 15;125:683–9.

49. Setayeshmehr M, Esfandiari E, Hashemibeni B, Tavakoli AH, Rafienia M, Samadikuchaksaraei A, et al. Chondrogenesis of human adipose-derived mesenchymal stromal cells on the [devitalized costal cartilage matrix/poly(vinyl alcohol)/fibrin] hybrid scaffolds. Eur Polym J. 2019 Sep 1;118:528–41.

50. Blackwood KA, McKean R, Canton I, Freeman CO, Franklin KL, Cole D, et al. Development of biodegradable electrospun scaffolds for dermal replacement. Biomaterials. 2008 Jul 1;29(21):3091–104.

51. Ma C, Huang DL, Chen HC, Chen DL, Xiong ZC. Preparation and characterization of electrospun poly (lactide-co-glycolide) membrane with different L-lactide and D-lactide ratios. J Polym Res. 2012 Feb 22;19(2):1–6.

52. Kubo M, Van De Water L, Plantefaber LC, Mosesson MW, Simon M, Tonnesen MG, et al. Fibrinogen and fibrin are anti-adhesive for keratinocytes: A mechanism for fibrin eschar slough during wound repair. J Invest Dermatol. 2001 Dec 1;117(6):1369–81.

53. Sese N, Cole M, Tawil B. Proliferation of Human Keratinocytes and Cocultured Human Keratinocytes and Fibroblasts in Three-Dimensional Fibrin Constructs. Tissue Eng Part A [Internet]. 2011 Feb 1 [cited 2020 Feb 19];17(3–4):429–37. Available from: https://www.liebertpub.com/doi/10.1089/ten.tea.2010.0113

54. Talens S, Leebeek FWG, Demmers JAA, Rijken DC. Identification of Fibrin Clot-Bound Plasma Proteins. Reitsma PH, editor. PLoS One [Internet]. 2012 Aug 3 [cited 2020 Feb 19];7(8):e41966. Available from: http://dx.plos.org/10.1371/journal.pone.0041966

55. Kim JP, Zhang K, Chen JD, Wynn KC, Kramer RH, Woodley DT. Mechanism of human keratinocyte migration on fibronectin: Unique roles of RGD site and integrins. J Cell Physiol [Internet]. 1992 Jun 1 [cited 2020 Feb 19];151(3):443–50. Available from: http://doi.wiley.com/10.1002/jcp.1041510303

56. Yamamoto M, Yanaga H, Nishina H, Watabe S, Mamba K. Fibrin Stimulates the

Proliferation of Human Keratinocytes through the Autocrine Mechanism of Transforming Growth Factor-α and Epidermal Growth Factor Receptor. Tohoku J Exp Med [Internet]. 2005 Sep [cited 2020 Feb 19];207(1):33–40. Available from: http://joi.jlc.jst.go.jp/JST.JSTAGE/tjem/207.33?from=CrossRef